Microscopic theory of in-plane critical field in two-dimensional Ising superconducting systems

Hongchao Liu,[1] Haiwen Liu,[2,*] Ding Zhang,[3,4] and X. C. Xie[1,4,5]

[1]*International Center for Quantum Materials, Peking University, Beijing 100871, China*

[2]*Department of Physics, Center for Advanced Quantum Studies, Beijing Normal University, Beijing 100875, China*

[3]*Department of Physics, State Key Laboratory of Low-Dimensional Quantum Physics, Tsinghua University, Beijing 100084, China*

[4]*Beijing Academy of Quantum Information Sciences, Beijing 100193, China*

[5]*CAS Center for Excellence in Topological Quantum Computation, University of Chinese Academy of Sciences, Beijing 100190, China*

(Received 28 July 2020; accepted 10 November 2020; published 24 November 2020)

We study the in-plane critical magnetic field of two-dimensional Ising superconducting systems and propose the microscopic calculation for these disordered two-dimensional superconducting systems with or without inversion symmetry. Protected by certain specific spin-orbit interaction which polarizes the electron spin to the out-of-plane direction, the in-plane critical fields largely surpass the Pauli limit and show remarkable upturn in the zero-temperature limit. The impurity scattering and Rashba spin-orbit interaction, treated on equal footing in the microscopic framework, both weaken the critical field but in qualitatively different manners. The microscopic theory is consistent with recent experimental results in stanene and Pb superconducting ultrathin films.

DOI: 10.1103/PhysRevB.102.174510

I. INTRODUCTION

The pair-breaking mechanisms of a conventional superconductor, such as scattering with paramagnetic impurities[1] as well as generation of vortices [2], have been intensively studied [3]. In layered superconductors, the reduction of dimensionality weakens the orbital effect when the magnetic field parallels the layered plane [4], therefore, providing a possible route to a large in-plane critical-field B_c. However, due to the Zeeman energy splitting, the Cooper pairs in conventional superconductors normally become unstable when the magnetic field exceeds the Pauli limit [5,6]. In contrast, the translational symmetry-breaking Fulde-Ferrell-Larkin-Ovchinnikov (FFLO) state can stabilize Cooper pairs beyond the Pauli limit [7,8] with the requirement that the superconductor locating in the clean limit [9,10]. Moreover, the spin-orbit scattering (SOS) randomizes the spin orientation by weakening the paramagnetism effect as shown in the Klemm-Luther-Beasley (KLB) theory and leads to enhancement of B_c [11]. Recent studies on two-dimensional (2D) crystalline superconductors [12–22] have pointed out yet a third mechanism to enhance B_c, originating from the spin-orbit interaction (SOI) of the system. The in-plane inversion symmetry breaking leads to out-of-plane polarization of electron spin, and the Cooper pairing is protected against the in-plane magnetic field [15–17]. The enhancement of critical field in inversion symmetry breaking Ising superconductors manifests as an important example of the general property in noncentrosymmetric superconductors [23]. Moreover, the enhanced critical fields are discussed theoretically and experimentally in systems locally lacking inversion symmetry [20,24] and proposed in layered superconductors with a competing pair-density-wave phase [25].

The impurity scattering will suppress any first-order phase transition or finite-momentum pairing [9,10,26], randomize the spin orientation, and, thus, renormalize the in-plane critical-field B_c. Moreover, apart from the aforementioned inversion-asymmetric Ising superconducting systems, certain inversion-symmetric 2D materials with spin splitting around the Γ point due to intrinsic spin-orbit interaction are very recently found capable of superconductivity [27–29]. A new microscopic model is needed to investigate the pair-breaking mechanism in these inversion-symmetric systems. And the combination effects of spin-orbit interaction and impurity scattering need to be studied on equal footing. Such investigations have been briefly mentioned by us on the recent discoveries of Ising superconducting systems with inversion symmetry [30,31] where they give quantitative explanations for the enhancement of in-plane B_c.

In this paper, we provide a more concrete and thorough analysis of our microscopic theory for 2D Ising superconductors with or without inversion symmetry and treat the Ising-inducing intrinsic SOI, the impurity scattering, and the Rashba SOI simultaneously. Starting from a schematic physical analysis, we propose a microscopic model and derive the in-plane critical-field relation $B_c(T)$ for inversion-symmetric Ising superconductivity and inversion-asymmetric one, respectively. The comparison of theoretical results with recent experiments is also given with a remarkable upturn at the zero-temperature limit, which is qualitatively different from the KLB formula.

II. INVERSION-SYMMETRIC ISING SUPERCONDUCTIVITY

This type of 2D superconductivity happens in a system with its energy valley at zero-momentum point Γ and two

*haiwen.liu@bnu.edu.cn

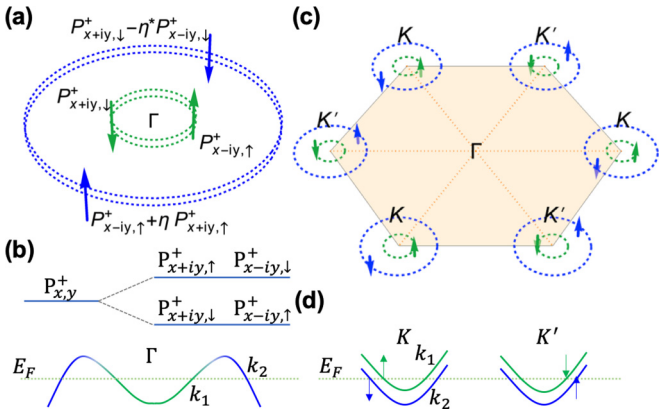

FIG. 1. Schematics of inversion-asymmetric and inversion-symmetric Ising superconductivity. (a) Two doubly degenerate FSs (green and blue dashed circle pairs) around the Γ point in the Brillouin zone of stanene (inversion-symmetric Ising). The arrows on the FSs denote spin directions along the $\pm z$ direction, k_1 in green, and k_2 in blue. Each FS is doubly degenerate, consisting of two different $P^+_{x,y}$ orbitals and out-of-plane spin directions. The pairing happens between $P^+_{x-iy,\uparrow}$ and $P^+_{x+iy,\downarrow}$ on the same FS if k_r is small (η cannot be neglected at large k_r and is explained in Discussions). (b) Fourfold degenerate $P^+_{x,y}$ level of stanene splits to two doubly degenerate levels due to SOI. The lower level forms two FSs at k_1 (green) and k_2 (blue). (c) Brillouin zone of ultrathin Pb film (inversion-asymmetric Ising) with double-nondegenerate FSs at each valley (green and blue dashed circles). Intervalley Cooper pairing form between electrons with the same color and opposite momentum. (d) Valley structure of Pb film in the vicinity of E_F. Each valley has two electron pockets, and Zeeman-type SOI polarizes electron spin oppositely around K and K'.

doubly degenerate Fermi surfaces (FSs) around it where the SOI is not Zeeman type. For example, in few-layer stanene, intrinsic SOI splits the fourfold degenerate $P^+_{x,y}$ level into two doubly degenerate levels, opening a gap at the Γ point [27,28]. The lower level crosses E_F at two different Fermi wave-vectors k_1, k_2, forming two different-shaped FSs [28], each of which holds two states [see Figs. 1(a) and 1(b)]. If the radius of the rth FS k_r is small, the eigenstates of the higher-energy level can be approximated by $P^+_{x+iy,\uparrow}, P^+_{x-iy,\downarrow}$, whereas those of the lower level can be approximated by $P^+_{x-iy,\uparrow}, P^+_{x+iy,\downarrow}$. Therefore, the SOI at valley Γ can be viewed as an out-of-plane magnetic field which takes opposite values $-B_{\rm eff}\hat{z}$ and $B_{\rm eff}\hat{z}$ on different orbits P^+_{x+iy} and P^+_{x-iy}, respectively ($\hat{z}$ is a unit vector perpendicular to the plane). In this way the system has time-reversal symmetry (TRS) at zero B, and electrons with opposite momenta and spins on the same isotropic FS can form s-wave Cooper pairs. The s-wave pairing with orbit-locked out-of-plane spin can give rise to the large in-plane B_c.

The double-FS structure of the inversion-symmetric Ising case differs from those of inversion-asymmetric Ising in their shape and location. Based on previous study [29], the system can be represented by a four-band model with basis $(P^+_{x+iy,\uparrow}, P^+_{x-iy,\uparrow}, P^+_{x-iy,\downarrow}, P^+_{x+iy,\downarrow})$ to describe the normal-state stanene with external in-plane magnetic-field $B\hat{x}$,

$$H_{II}(\boldsymbol{k}) = Ak^2 + \begin{bmatrix} H_+(\boldsymbol{k}) & -\mu_B B\sigma_x \\ -\mu_B B\sigma_x & H_-(\boldsymbol{k}) \end{bmatrix}, \quad (1)$$

$$H_\pm(\boldsymbol{k}) = \begin{bmatrix} M_0 - M_1k^2 & v(\pm k_x - ik_y) \\ v(\pm k_x + ik_y) & -M_0 + M_1k^2 \end{bmatrix}, \quad (2)$$

with A, M_0, M_1, v as fitting parameters, and μ_B as the effective Bohr magneton. H_{II} has TRS at $B = 0$. There are two isotropic dispersion relations,

$$E_\pm(k) = Ak^2 \pm \sqrt{(M_0 - M_1k^2)^2 + v^2k^2 + \mu_B^2B^2}, \quad (3)$$

each of which is doubly degenerate. At small k and $B = 0$, the degenerate eigenstates of $E_-(k)$ can be approximated by $P^+_{x-iy,\uparrow}, P^+_{x+iy,\downarrow}$. We consider the lower-band $E_-(k)$ crossing E_F at two different Fermi wave-vectors k_1 and k_2 [see Fig. 1(b)] and take into account the spin-independent scattering disorder within each FS by setting a mean free time τ_0 in the Green's function [2,32,33]. The critical field for each FS can be solved within the Werthamer-Helfand-Hohenberg (WHH) framework [2,33] and be joined together in light of quasiclassical two-band Usadel equations [33,34]. The critical field satisfies

$$\frac{2w}{\lambda_0}F(\tilde{m}_1,t,b)F(\tilde{m}_2,t,b) + \left(1+\frac{\lambda_-}{\lambda_0}\right)F(\tilde{m}_1,t,b) + \left(1-\frac{\lambda_-}{\lambda_0}\right)F(\tilde{m}_2,t,b) = 0, \quad (4)$$

where the subscripts $r = 1, 2$ label the two bands, $\lambda_{rr'}$ is the matrix of BCS coupling constants (assumed $\lambda_{11} > \lambda_{22}$), $\lambda_\pm = \lambda_{11} \pm \lambda_{22}$, $\lambda_0 = \sqrt{\lambda_-^2 + 4\lambda_{12}^2}$, $w = \lambda_{11}\lambda_{22} - \lambda_{12}^2$,

$$F(\tilde{m}_r,t,b) \equiv \ln t + \frac{b^2}{\tilde{m}_r^2 + b^2} \times \left[\mathrm{Re}\psi\left(\frac{1}{2} + \frac{i\sqrt{\tilde{m}_r^2+b^2}}{2\pi t}\right) - \psi\left(\frac{1}{2}\right)\right],$$

$$\tilde{m}_r = \frac{\sqrt{(M_0 - M_1k_r^2)^2 + v^2k_r^2}}{k_BT_c + \hbar/(2\pi\tau_0)},$$

$$t = \frac{T}{T_c},$$

$$b = \frac{\mu_B B_c}{k_BT_c}, \quad (5)$$

$\psi(x)$ is the digamma function, $\tilde{m}_r$ is the effective SOI, and all the functions and parameters appearing in Eqs. (4) and (5) are dimensionless. When the two FSs have analogous shapes ($\tilde{m}_1 \approx \tilde{m}_2$), or interlayer coupling is very weak ($\lambda_{12} \ll \lambda_-$), Eq. (4) has a simpler one-band form $F(\tilde{m}_1,t,b) = 0$. Meanwhile, in the more generic situation, influenced by both bands, the Eq. (4) cannot be simplified with the curve of inversion-symmetric Ising case deviating from $F(\tilde{m}_1,t,b) = 0$.

Near T_c, the inversion-symmetric Ising formalism is consistent with the 2D in-plane field Ginzburg-Landau (2D-GL) theory [35] and the KLB theory [11]. As shown in Fig. 2(b) we compare the inversion-symmetric Ising case with 2D-GL

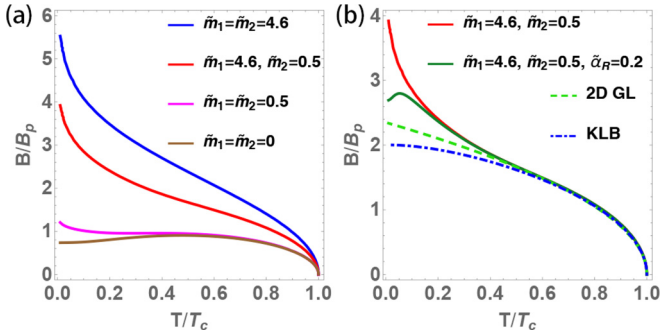

FIG. 2. In-plane critical field normalized by B_p as a function of temperature normalized by T_c. (a) Inversion-symmetric Ising theory Eq. (4) (red curve) and its special cases $\tilde{m}_1 = \tilde{m}_2 \neq 0$ (blue and pink), and the zero SOI trivial case $\tilde{m}_1 = \tilde{m}_2 = 0$ (brown). The common parameters not showing in the legend are taken as $\lambda_{11} = 3,\ \lambda_{22} = 1,\ \lambda_{12} = 2$. (b) Inversion-symmetric Ising (red), inversion-symmetric Ising with Rashba-type SOI (dark green), 2D-GL theory, and KLB theory. $\tilde{\alpha}_R$ is the effective Rashba SOI, and parameters of 2D-GL and KLB theory are $\xi_{GL}d_{sc} = \frac{0.88\hbar}{eB_p},\ \tau_{so}^{-1} = 9.9k_BT_c$.

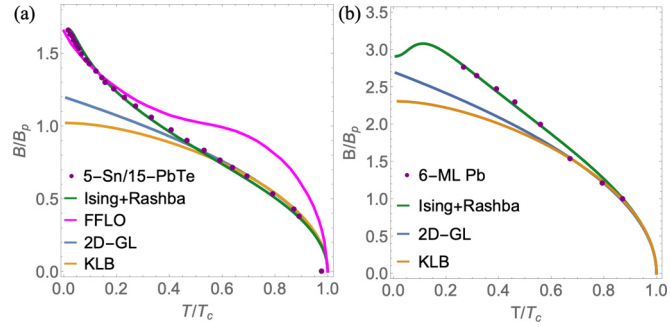

FIG. 3. Normalized in-plane critical-field B/B_p as a function of reduced temperature T/T_c in different types of Ising superconducting systems. (a) Few-layer stanene 5-Sn/15-PbTe, $T_c = 1.25$ K, and $B_p = 2.33$ T, fitted by inversion-symmetric Ising theory, and the experimental data are from Ref. [30]. The fitting shows a weak Rashba parameter $\tilde{\alpha}_R = 0.06$ compared with the Ising parameter $\tilde{m}_1 = 3.76$ for k_1 FS, and the k_2 FS has $\tilde{m}_2 = 0$ possibly because k_2 is too large. The BCS coupling constants are $\lambda_{11} = 3,\ \lambda_{22} = 0.65,\ \lambda_{12} = 0.5$. The FFLO, 2D-GL, and KLB theoretical curves are also given for comparison. (b) Six-monolayer (ML) Pb films, $T_c = 6.00$ K and $B_p = 14.7$ T, fitted by inversion-asymmetric Ising theory with $\tilde{\beta}_{so} = 5.80,\ \tilde{\alpha}_R = 0.40$, and the experimental data are from Ref. [18]. The 2D-GL and KLB theoretical curves are also given for comparison. For lack of low-T data in Pb film experiments, FFLO theory is irrelevant and, thus, not shown.

theory [35],

$$B_c = \frac{\sqrt{12}}{2\pi}\frac{\Phi_0}{\xi_{GL}d_{sc}}\sqrt{1-\frac{T}{T_c}}, \tag{6}$$

and KLB theory of the SOS mechanism [11,36],

$$\ln\frac{T}{T_c} + \psi\left(\frac{1}{2}+\frac{3\tau_{so}}{2\hbar}\frac{\mu_B^2B_c^2}{2\pi k_BT}\right) - \psi\left(\frac{1}{2}\right) = 0. \tag{7}$$

Here Φ_0, ξ_{GL}, d_{sc}, and τ_{so} denote the flux quantum, the GL coherence length at zero temperature, the effective thickness of superconductivity, and the SOS time, respectively. When the temperature is near T_c, the $B_c(T)$ relations predicted in Eqs. (4) and (7) are both proportional to $\sqrt{1-T/T_c}$, consistent with 2D-GL theory.

In the low-temperature region, inversion-symmetric Ising theory has an apparently larger field than 2D-GL, the KLB theory, and the zero SOI case. Moreover, it has a remarkable upturn near the zero temperature. This upturn establishes a stark difference from the standard pair-breaking (SPB) theory discussed by Fulde [3], Fulde *et al.* [37], and Fulde [38]. Various TRS-breaking cases lead to the same equation and similar thermodynamics properties, and TRS-breaking factors function as a generic parameter in that equation. If the TRS-breaking factor is the field B_c, and the equation of SPB theory is

$$\ln\frac{T}{T_c} + \mathrm{Re}\,\psi\left(\frac{1}{2}+\frac{\hbar}{\tau_{\mathcal{R}}(B_c)}\frac{1}{2\pi k_BT}\right) - \psi\left(\frac{1}{2}\right) = 0, \tag{8}$$

where $\tau_{\mathcal{R}}(B_c)$ is a function of B_c acting as the generic TRS-breaking parameter with a real or complex value. From Eq. (8), one can obtain $\lim_{T\to 0}|\tau_{\mathcal{R}}(B_c)| = \frac{2e^{\gamma}}{\pi}\frac{\hbar}{k_BT_c}$, where $\gamma = 0.577$ is the Euler constant. If we set $|\tau_{\mathcal{R}}(B_c)| = \frac{\hbar}{\mu_BB_c}$ or $|\tau_{\mathcal{R}}(B_c)| = \frac{2}{3\tau_{so}}(\frac{\hbar}{\mu_BB_c})^2$ in Eq. (8), we reach the zero SOI case $F(0,t,b) = 0$ or KLB theory Eq. (7). Therefore, the critical field near $T = 0$ in those two situations is asymptotic to some finite constant, and no upturn can happen. However, Eq. (4) shows remarkable upturn in the low-temperature region, which is indeed a distinguished experimental property of inversion-symmetric Ising superconductivity [30]. Although the FFLO state also shows upturn B_c in the low-temperature region, however, the impurity scattering can destroy the finite-momentum Cooper pairs [9,10]. Moreover, the upturn feature in the low-temperature region is quantitatively different from the FFLO state [see Fig. 3(a)].

The upturn can be explained from the two-level structure of the four-band model Eq. (1). In Fig. 1(b), we plot the schematic of energy levels at the Γ point, and the electrons on E_- ($P^+_{x-iy,\uparrow}$ or $P^+_{x+iy,\downarrow}$) can be excited to E_+ ($P^+_{x-iy,\downarrow}$ or $P^+_{x+iy,\uparrow}$) by thermal activation or parallel magnetic field. In the high-temperature region, both levels are partially filled, so the superposition of up-spin and down-spin of the same orbit P^+_{x+iy} (or P^+_{x-iy}) weakens the spin polarization along the z direction and the phenomena is like 2D-GL and KLB theory. By contrast if T is close to zero, the upper band is almost empty, so its influence is negligible, and the electrons have robust spin polarization, making the Cooper pairing very difficult to break by the parallel field and leading to the upturn of B_c in the low-temperature region.

III. INVERSION-ASYMMETRIC ISING SUPERCONDUCTIVITY

For in-plane inversion-asymmetric systems, the inversion-asymmetric Ising superconductivity is caused by Zeeman-type SOI. Considering the 2D hexagonal lattice as an example, the SOI serves as an out-of-plane magnetic field which takes the opposite value $B_{\mathrm{eff}}\hat{z}$, $-B_{\mathrm{eff}}\hat{z}$ at valleys K and K', and the spin degeneracies of energy bands are lifted,

resulting in double-FSs with almost the same radius and shape around each valley [see Fig. 1(d)]. Thus, electrons at $\boldsymbol{K}+\boldsymbol{k}_r$ and $-\boldsymbol{K}-\boldsymbol{k}_r$ ($r=1,2$ labels the two FSs) have opposite out-of-plane spin because of TRS [see Fig. 1(c)], and intervalley Cooper pairs formed by those electrons are stable under an in-plane field much larger than B_p. When an in-plane magnetic-field $B\hat{x}$ is present, the normal-state Hamiltonian reads $H_I(k)=\frac{\hbar^2k^2}{2m}-\beta_{so}\sigma_z\tau_z-\mu_B B\sigma_x$ [39], where m is the effective mass, σ and τ denote the real spin subspace and valley subspace, respectively. The relation between critical-field B_c and temperature T can be solved within the WHH framework [18], and the in-plane critical field satisfies the equation,

$$\ln\left(\frac{T_c}{T}\right)=\sum_{n=0}^{\infty}\frac{2\pi k_BT\mu_B^2B_c^2}{\omega_n\left[\omega_n^2+\frac{\beta_{so}^2}{(1+\hbar/2\omega_n\tau_0)^2}+\mu_B^2B_c^2\right]}, \tag{9}$$

with Matsubara frequencies $\omega_n=(2n+1)\pi k_BT$ and spin-independent scattering τ_0. If the spin-independent scattering is weak, or the temperature is not too low, the simplified equation is $F(\tilde{\beta}_{so},t,b)=0$ in terms of dimensionless effective Zeeman-type SOI $\tilde{\beta}_{so}=\frac{\beta_{so}}{k_BT_c+\hbar/(2\pi\tau_0)}$. Instead of using the Dyson equations technique to solve the inversion-asymmetric problem [40], the WHH method here finishes the work after the fashion of the aforementioned inversion-symmetric Ising case, showing its convenience in both types of Ising superconductivity. We note that when Eq. (4) of inversion symmetric returns to $F(\tilde{m}_1,t,b)=0$, the functional form looks like the inversion-asymmetric Ising case, but the new effective parameter $\tilde{m}_1$ is not the Zeeman-type SOI. This similarity in mathematical form suggests the universality of the $F(\tilde{m},t,b)$ function in various types of Ising superconductivity.

IV. DISCUSSIONS

There may be multiple types of SOI working simultaneously, including the Ising-inducing SOI and the Rashba SOI to affect the in-plane B_c in experiments [15,16]. Considering the effect of Rashba SOI originating from the interface, both the inversion-symmetric formula Eqs. (4) and (5) and the inversion-asymmetric formula Eq. (9) can be further modified to include the influence of Rashba SOI and be utilized to fit the in-plane critical-field B_c of few-layer stanene and ultrathin crystalline Pb films, respectively [33]. In both cases, the weak Rashba-type SOI tends to polarize the spin to the in-plane direction, making the Cooper pairs more susceptible to the in-plane magnetic field. We use both types of formulas for Ising superconductivity with dimensionless effective Rashba-type SOI $\tilde{\alpha}_R=\frac{\alpha_Rk_F/\sqrt{2}}{k_BT_c+\hbar/(2\pi\tau_0)}$ to fit the experimental data quantitatively [see Fig. 3], and the results give very weak Rashba-type SOI parameter $\tilde{\alpha}_R\ll\tilde{m}_1$ or $\tilde{\alpha}_R\ll\tilde{\beta}_{so}$. The weak Rashba-type SOI may destruct the upturn or even causes a downturn at the zero-temperature limit [see Figs. 2(b) and 3(b)]. The experimental data points in Fig. 3(b) lack data at the zero-temperature limit, possibly because the large $B_c(T)$ is beyond the present experimental feasible regime, but we expect a saturation or downturn in this limit in future experiments.

In the above derivation, changing the disorder strength renormalizes every effective SOI parameter in the same way $\tilde{X}=\frac{X_0}{1+\hbar/(2\pi\tau_0k_BT_c)}$, where $X=m_1,m_2,\beta_{so},\alpha_R$ and X_0 denotes the original dimensionless SOI. Therefore, the curves in Fig. 4 of smaller τ_0 give smaller $B_c(T)$ for any $T<T_c$ because of smaller $\tilde{m}_1,\tilde{m}_2$, meanwhile the effect of Rashba SOI is weaker. The solid lines in Fig. 4 overlap more with the dashed ones for smaller τ_0, showing the Rashba effect strongly restricted in a narrower low-temperature region as the system gets dirtier.

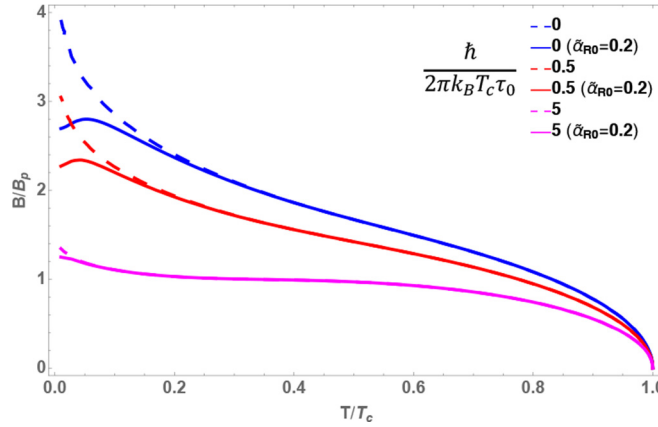

FIG. 4. In-plane critical field normalized by B_p as a function of temperature normalized by T_c for inversion-symmetric Ising formula Eq. (4). The solid lines are the B_c-T relations with Rashba SOI, and the dashed lines are those without Rashba SOI. The SOI parameters are the same for all curves $m_{1,0}=4.6$, $m_{2,0}=0.5$, and $\alpha_{R0}=0.2$, whereas the values of τ_0 are different. The BCS coupling constants are $\lambda_{11}=3$, $\lambda_{22}=1$, $\lambda_{12}=2$.

It should be noted that the Hamiltonian model Eq. (1) for inversion-symmetric Ising theory is block diagonal at zero B, and the eigenstates at the rth FS can be written as $P^+_{x-iy,\uparrow}+\eta P^+_{x+iy,\uparrow}$ and $P^+_{x+iy,\downarrow}-\eta^*P^+_{x-iy,\downarrow}$, where $|\eta|=vk_r/2M_0+O(k_r^2)$. If k_r is close to zero, then the eigenstates can be approximated by $P^+_{x-iy,\uparrow}$ and $P^+_{x+iy,\downarrow}$, and the SOI can be viewed as a result of orbit-locked $\pm B_{\rm eff}\hat{z}$ mentioned before [see Fig. 1(d)]. If k_r is too large, the coupling parameter η cannot be neglected, which gives rise to smearing out of Ising pairing. In other words, the effect of η is similar to that of the Rashba SOI, and, thus, can also contribute to bend downward the critical field at the zero-temperature limit.

V. SUMMARY

We propose the microscopic theory for the in-plane critical field of two-dimensional Ising superconducting systems, including systems with or without inversion symmetry breaking. In both systems, the intrinsic spin-orbit interaction polarizes the electron spin to the out-of-plane direction, which gives rise to a large in-plane critical field surpassing the Pauli limit. Meanwhile, the critical field shows remarkable upturn near the zero-temperature limit. The microscopic theory can quantitatively explain recent experimental results in stanene and Pb superconducting ultrathin films.

ACKNOWLEDGMENTS

Hongchao Liu is grateful for J. Wang and Y. Liu for their insightful discussions throughout the previous collaborations on related works. This work was financially supported by

the National Basic Research Program of China (Grants No. 2017YFA0303301 and No. 2015CB921102), the National Natural Science Foundation of China (Grants No. 11674028, No. 11534001, and No. 11504008).

[1] A. A. Abrikosov and L. P. Gor'kov, Contribution to the theory of superconducting alloys with paramagnetic impurities, Sov. Phys. JETP **12**, 1243 (1961).

[2] N. R. Werthamer, E. Helfand, and P. C. Hohenberg, Temperature and purity dependence of the superconducting critical field, H_{c2}. iii. electron spin and spin-orbit effects, Phys. Rev. **147**, 295 (1966).

[3] P. Fulde, Cooper pair breaking, in *BCS: 50 years*, edited by L. N. Cooper and D. Feldman (World Scientific, Singapore, 2010) Chap. 11, pp. 227–254.

[4] M. Tinkham, *Introduction to Superconductivity* (McGraw-Hill, New York, 1996).

[5] B. Chandrasekhar, A note on the maximum critical field of high-field superconductors, Appl. Phys. Lett. **1**, 7 (1962).

[6] A. M. Clogston, Upper Limit for the Critical Field in Hard Superconductors, Phys. Rev. Lett. **9**, 266 (1962).

[7] P. Fulde and R. A. Ferrell, Superconductivity in a strong spin-exchange field, Phys. Rev. **135**, A550 (1963).

[8] A. I. Larkin and Y. N. Ovchinnikov, Inhomogeneous state of superconductors, Sov. Phys. JETP. **20**, 762 (1965).

[9] Y. Matsuda and H. Shimahara, Fulde-Ferrell-Larkin-Ovchinnikov state in heavy fermion superconductors, J. Phys. Soc. Jpn. **76**, 051005 (2007).

[10] J. Wosnitza, FFLO states in layered organic superconductors, Ann. Phys. (Berl.) **530**, 1700282 (2017).

[11] R. A. Klemm, A. Luther, and M. R. Beasley, Theory of the upper critical field in layered superconductors, Phys. Rev. B **12**, 877 (1975).

[12] Y. Saito, T. Nojima, and Y. Iwasa, Highly crystalline 2d superconductors, Nat. Rev. Mater. **2**, 16094 (2017).

[13] Y. Saito, Y. Kasahara, J. Ye, Y. Iwasa, and T. Nojima, Science **350**, 409 (2015).

[14] Y. Xing, H.-M. Zhang, H.-L. Fu, H. Liu, Y. Sun, J.-P. Peng, F. Wang, X. Lin, X.-C. Ma, Q.-K. Xue, J. Wang, and X. C. Xie, Quantum Griffiths singularity of superconductor-metal transition in Ga thin films, Science **350**, 542 (2015).

[15] J. Lu, O. Zheliuk, I. Leermakers, N. F. Yuan, U. Zeitler, K. T. Law, and J. Ye, Evidence for two-dimensional Ising superconductivity in gated MoS_2, Science **350**, 1353 (2015).

[16] Y. Saito, Y. Nakamura, M. S. Bahramy, Y. Kohama, J. Ye, Y. Kasahara, Y. Nakagawa, M. Onga, M. Tokunaga, T. Nojima, Y. Yanase, and Y. Iwasa, Superconductivity protected by spin–valley locking in ion-gated MoS_2, Nat. Phys. **12**, 144 (2016).

[17] X. Xi, Z. Wang, W. Zhao, J.-H. Park, K. T. Law, H. Berger, L. Forró, J. Shan, and K. F. Mak, Ising pairing in superconducting $NbSe_2$ atomic layers, Nat. Phys. **12**, 139 (2016).

[18] Y. Liu, Z. Wang, X. Zhang, C. Liu, Y. Liu, Z. Zhou, J. Wang, Q. Wang, Y. Liu, C. Xi, M. Tian, H. Liu, J. Feng, X. C. Xie, and J. Wang, Interface-Induced Zeeman-Protected Superconductivity in Ultrathin Crystalline Lead Films, Phys. Rev. X **8**, 021002 (2018).

[19] J. Lu, O. Zheliuk, Q. Chen, I. Leermakers, N. E. Hussey, U. Zeitler, and J. Ye, Full superconducting dome of strong Ising protection in gated monolayer WS_2, Proc. Natl. Acad. Sci. USA **115**, 3551 (2018).

[20] S. C. de la Barrera, M. R. Sinko, D. P. Gopalan, N. Sivadas, K. L. Seyler, K. Watanabe, T. Taniguchi, A. W. Tsen, X. Xu, D. Xiao, and B. M. Hunt, Tuning Ising superconductivity with layer and spin-orbit coupling in two-dimensional transition-metal dichalcogenides, Nat. Commun. **9**, 1427 (2018).

[21] Y. Liu, Z. Wang, P. Shan, Y. Tang, C. Liu, C. Chen, Y. Xing, Q. Wang, H. Liu, X. Lin, X. C. Xie, and J. Wang, Anomalous quantum Griffiths singularity in ultrathin crystalline lead films, Nat. Commun. **10**, 3633 (2019).

[22] N. F. Q. Yuan, B. T. Zhou, W.-Y. He, and K. T. Law, Ising Superconductivity in Transition Metal Dichalcogenides, arXiv:1605.01847.

[23] *Non-Centrosymmetric Superconductors: Introduction and Overview*, edited by E. Bauer and M. Sigrist, Lecture Notes in Physics Vol. 847 (Springer, Berlin, Heidelberg, 2012).

[24] S. J. Youn, M. H. Fischer, S. H. Rhim, M. Sigrist, and D. F. Agterberg, Role of strong spin-orbit coupling in the superconductivity of the hexagonal pnictide SrPtAs, Phys. Rev. B **85**, 220505(R) (2012).

[25] D. Möckli, Y. Yanase, and M. Sigrist, Orbitally limited pair-density-wave phase of multilayer superconductors, Phys. Rev. B **97**, 144508 (2018).

[26] M. Aizenman and J. Wehr, Rounding of First-Order Phase Transitions in Systems with Quenched Disorder, Phys. Rev. Lett. **62**, 2503 (1989).

[27] Y. Xu, B. Yan, H.-J. Zhang, J. Wang, G. Xu, P. Tang, W. Duan, and S.-C. Zhang, Large-Gap Quantum Spin Hall Insulators in Tin Films, Phys. Rev. Lett. **111**, 136804 (2013).

[28] M. Liao, Y. Zang, Z. Guan, H. Li, Y. Gong, K. Zhu, X.-P. Hu, D. Zhang, Y. Xu, Y.-Y. Wang, K. He, X.-C. Ma, S.-C. Zhang, and Q.-K. Xue, Superconductivity in few-layer stanene, Nat. Phys. **14**, 344 (2018).

[29] C. Wang, B. Lian, X. Guo, J. Mao, Z. Zhang, D. Zhang, B.-L. Gu, Y. Xu, and W. Duan, Type-II Ising Superconductivity in Two-Dimensional Materials with Spin-Orbit Coupling, Phys. Rev. Lett. **123**, 126402 (2019).

[30] J. Falson, Y. Xu, M. Liao, Y. Zang, K. Zhu, C. Wang, Z. Zhang, H. Liu, W. Duan, K. He, H. Liu, J. H. Smet, D. Zhang, and Q.-K. Xue, Type-II Ising pairing in few-layer stanene, Science **367**, 1454 (2020).

[31] Y. Liu, Y. Xu, J. Sun, C. Liu, Y. Liu, C. Wang, Z. Zhang, K. Gu, Y. Tang, C. Ding, H. Liu, H. Yao, X. Lin, L. Wang, Q.-K. Xue, and J. Wang, Type-II Ising Superconductivity and Anomalous Metallic State in Macro-Size Ambient-Stable Ultrathin Crystalline Films, Nano Lett. **20**, 5728 (2020).

[32] A. A. Abrikosov, L. P. Gorkov, and I. E. Dzyaloshinski, *Methods of Quantum Field Theory in Statistical Physics* (Prentice-Hall, Englewood Cliffs, NJ, 1963).

[33] See Supplemental Material at http://link.aps.org/supplemental/10.1103/PhysRevB.102.174510, which includes Refs. [41,42] for detailed microscopic calculations.

[34] A. Gurevich, Enhancement of the upper critical field by nonmagnetic impurities in dirty two-gap superconductors, Phys. Rev. B **67**, 184515 (2003).

[35] M. Tinkham, Effect of fluxoid quantization on transitions of superconducting films, Phys. Rev. **129**, 2413 (1963).

[36] P. M. Tedrow and R. Meservey, Critical magnetic field of very thin superconducting aluminum films, Phys. Rev. B **25**, 171 (1982).

[37] P. Fulde, L. Hirst, and A. Luther, Superconductors containing impurities with crystal-field split energy levels, Z. Phys. **230**, 155 (1970).

[38] P. Fulde, Crystal fields, in *Handbook on the Physics and Chemistry of Rare Earths*, edited by K. A. Gschneidner and L. Eyring (North-Holland, Amsterdam, 1979) Chap. 17, pp. 295–386.

[39] N. F. Q. Yuan, K. F. Mak, and K. T. Law, Possible Topological Superconducting Phases of MoS_2, Phys. Rev. Lett. **113**, 097001 (2014).

[40] S. Ilić, J. S. Meyer, and M. Houzet, Enhancement of the Upper Critical Field in Disordered Transition Metal Dichalcogenide Monolayers, Phys. Rev. Lett. **119**, 117001 (2017).

[41] H. Shimahara, Fulde-ferrell state in quasi-two-dimensional superconductors, Phys. Rev. B **50**, 12760 (1994).

[42] G. Zwicknagl, S. Jahns, and P. Fulde, Critical magnetic field of ultra-thin superconducting films and interfaces, J. Phys. Soc. Jpn. **86**, 083701 (2017).